The contribution of vascular and extra-vascular water pathways to drought-induced decline of leaf hydraulic conductance

Patrizia Trifiló[1,*], Fabio Raimondo[1], Tadeja Savi[2], Maria A. Lo Gullo[1] and Andrea Nardini[2]

[1] Dipartimento di Scienze Chimiche, Biologiche, Farmaceutiche e Ambientali, Università di Messina, Salita F. Stagno D'Alcontres 31, 98166 Messina, Italy
[2] Dipartimento di Scienze della Vita, Università di Trieste, Via L. Giorgieri 10, 34127 Trieste, Italy

* Correspondence: ptrifilo@unime.it

Accepted 20 June 2016

Abstract

Drought stress can impair leaf hydraulic conductance (K_{leaf}), but the relative contribution of changes in the efficiency of the vein xylem water pathway and in the mesophyll route outside the xylem in driving the decline of K_{leaf} is still debated. We report direct measurements of dehydration-induced changes in the hydraulic resistance (R=1/K) of whole leaf (R_{leaf}), as well as of the leaf xylem (R_x) and extra-vascular pathways (R_{ox}) in four Angiosperm species. R_{leaf}, R_x, and R_{ox} were measured using the vacuum chamber method (VCM). R_{leaf} values during progressive leaf dehydration were also validated with measurements performed using the rehydration kinetic method (RKM). We analysed correlations between changes in R_x or R_{ox} and R_{leaf}, as well as between morpho-anatomical traits (including dehydration-induced leaf shrinkage), vulnerability to embolism, and leaf water relation parameters. Measurements revealed that the relative contribution of vascular and extra-vascular hydraulic properties in driving K_{leaf} decline during dehydration is species-specific. Whilst in two study species the progressive impairment of both vascular and extra-vascular pathways contributed to leaf hydraulic vulnerability, in the other two species the vascular pathway remained substantially unaltered during leaf dehydration, and K_{leaf} decline was apparently caused only by changes in the hydraulic properties of the extra-vascular compartment.

Key words: Drought, leaf extra-vascular conductance, leaf hydraulic conductance, leaf vein conductance, leaf vulnerability, shrinkage, vulnerability segmentation.

Introduction

Plant survival and productivity are assured by CO_2 uptake through stomata and photosynthetic carbon fixation. Both processes mainly occur at the leaf level, and are critically dependent on plant water status, and specifically on leaf water balance. In fact, any reduction in leaf water supply with respect to evaporative demand may induce stomatal closure and reduction of photosynthetic rates (Sperry, 2000).

Leaves represent the terminal part of the soil–plant–atmosphere continuum. The water potential difference between leaf and atmosphere drives water loss by evaporative processes, and ultimately generates the driving force for water uptake at the root level and long-distance transport through stems and up to the leaf evaporation sites. Hence, the efficiency of the water transport through the plant (hydraulic conductance,

K_{plant}) is a key parameter affecting plant photosynthesis and productivity (Santiago *et al.*, 2004; Brodribb *et al.*, 2005). Plant hydraulic resistance (R_{plant}=1/K_{plant}) is strongly influenced by leaf hydraulic properties, and in fact leaf hydraulic resistance (R_{leaf}=1/K_{leaf}) contributes 30% or more of R_{plant}, thus representing a major bottleneck of the plant hydraulic system (Sack and Holbrook, 2006).

Leaf hydraulics are complex, as two major pathways and associated resistances co-limit water transport in this organ, i.e. the vein xylem system (R_x) and the mesophyll route outside the xylem (R_{ox}) (Buckley *et al.*, 2015). Water enters the petiole and moves through veins up to bundle sheath cells (Nardini *et al.*, 2010). At the bundle sheath level, water exits the xylem and travels to mesophyll cells along different routes comprising symplastic, apoplastic, and gas phase pathways (Buckley, 2015). The hydraulic resistances of the vascular and extra-vascular pathways are generally reported to be of the same order of magnitude (Nardini *et al.*, 2005; Sack *et al.*, 2005), although some studies have suggested dominance of the extra-vascular resistance over the vascular one (Cochard *et al.*, 2004; Gascò *et al.*, 2004).

The leaf vascular resistance is governed by vein xylem traits such as conduit lumen, vein length per unit area, hierarchy, tapering, and topology (Sack and Scoffoni, 2013; Xiong *et al.*, 2015). Hence, short-to-mid-term changes in R_x within a plant may arise in response to mechanical damage (Nardini and Salleo, 2003; Sack *et al.*, 2008) or as a consequence of drought-induced xylem embolism (Nardini *et al.*, 2001; Trifilò *et al.*, 2003*b*; Johnson *et al.*, 2009*a*). By contrast, the extra-vascular component is a micro-hydraulic system more complex and dynamic than the vascular one. R_{ox} depends on structural traits such as shape and size of mesophyll cells (Buckley *et al.*, 2015), but can be modulated by changes in expression/activity of aquaporins in response to light, water stress, and other environmental factors (Heinen *et al.*, 2009; Voicu *et al.*, 2009; Miniussi *et al.*, 2015), and even by changes in the efficiency of the gas phase pathway (Buckley *et al.*, 2015). For example, high temperature gradients within the leaves have been reported to increase vapor phase transport (Rockwell *et al.*, 2014; Buckley, 2015).

Several studies have shown that drought stress can lead to important reductions of K_{leaf} (Brodribb and Holbrook, 2006; Scoffoni *et al.*, 2012) with consequent impacts on gas exchange and photosynthesis (Lo Gullo *et al.*, 2003). However, the mechanistic link between K_{leaf} drop and associated changes in R_x and R_{ox} is still a matter of debate. Drought stress causes a reduction of leaf water potential and xylem pressure, thus potentially leading to vein xylem embolism and increased R_x. The occurrence of xylem embolism events in leaf veins has been recorded via acoustic methods (Kikuta *et al.*, 1997; Nardini *et al.*, 2001), hydraulic measurements (Nardini *et al.*, 2008; Charra-Vaskou *et al.*, 2012), and direct visualization of vein blockage (Salleo *et al.*, 2003; Brodribb *et al.*, 2016; Ryu *et al.*, 2016). On the other hand, the role of changes in R_{ox} in determining the drop of K_{leaf} upon leaf dehydration is much less understood, despite recent research efforts in this direction. As an example, Charra-Vaskou *et al.* (2012) reported that drought-induced decline of needle hydraulic conductance in *Pinus pinaster* was mostly due to changes in the hydraulic properties of the extra-vascular tissues. Across different Angiosperm species, leaf hydraulic vulnerability, expressed as the leaf water potential inducing 50% loss of K_{leaf} (P_{50}) is generally correlated to leaf water potential at the turgor loss point (Ψ_{tlp}) (Blackman *et al.*, 2010; Nardini *et al.*, 2012*a*; Nardini and Luglio, 2014). While such a correlation might simply reflect the co-ordination of functional traits conferring drought resistance at the apoplastic and symplastic levels, recent experimental evidence suggests that the link between P_{50} and Ψ_{tlp} might also have a mechanistic basis. Indeed, Martorell *et al.* (2015) have reported that P_{50} of grapevine leaves changes on a seasonal basis in parallel with changes in Ψ_{tlp}, suggesting that osmotic adjustment mediates the plasticity of leaf hydraulic vulnerability. Decreased Ψ_{tlp} during drought periods would assure maintenance of cell turgor, thus preventing cell shrinkage and consequent impacts on R_{ox}. Alternatively, changes in cell turgor might mediate aquaporin activity (Kim and Steudle, 2007), again with effects on extra-vascular hydraulic properties. This scenario is also supported by recent studies (Scoffoni *et al.*, 2014) reporting striking correlations of drought-induced decline of K_{leaf} with leaf shrinkage, as well as between leaf shrinkage and leaf water relation parameters such as osmotic potential and modulus of elasticity across 14 species. A close correlation between leaf shrinkage and K_{leaf} decline under water stress has been recently confirmed for *Salvia officinalis* by Savi *et al.* (2016), and fast recovery of K_{leaf} in this species upon rehydration was in fact attributed to cell turgor recovery, in contrast with other studies suggesting that fast and reversible changes of K_{leaf} might arise from cycles of embolism formation and recovery (Trifilò *et al.*, 2003*a*; Johnson *et al.*, 2009*b*; Laur and Hacke, 2014).

Clearly, the relative contribution of changes in R_x and R_{ox} in driving the decline of K_{leaf} under drought stress is still unresolved. Moreover, it can be hypothesized that the relative importance of vein xylem embolism versus loss of cell turgor and shrinkage as factors affecting leaf hydraulics during water stress and recovery might even be somehow species-specific, as already shown for the basic partitioning of hydraulic resistances between the vascular and extra-vascular compartments (Sack *et al.*, 2005). In this study, we present experimental data gathered on leaves of four Angiosperm species. Our aim was to experimentally measure changes of R_x and R_{ox} during leaf dehydration, and correlate these changes with the overall drop of K_{leaf}. Moreover, we tested possible correlations between changes in K_{leaf} and other leaf physiological properties including vulnerability to shrinkage under drought and leaf water relation parameters.

Material and methods

Experiments were performed between May and October 2014 on two evergreen (*Aleurites moluccana* L. [Willd] and *Magnolia grandiflora* L.) and two deciduous (*Quercus rubra* L. and *Vitis labrusca* L.) species (Table 1). Species were selected to cover a wide range of values of leaf mass per area (LMA) (see Results). Leaves were sampled from two plants per species. All plants were about 15–20 years old, and were growing in the campus of the University of Messina.

Table 1. *List of the species under study and abbreviations used in tables and figures. For each species, the family, native region and corresponding climate zone, habitus, and growth form are reported*

Species	Family	Origin	Climate zone	Habitus	Growth form
Aleurites moluccana (*Am*)	Euphorbiaceae	Indo-Malayan	Tropical	Evergreen	Tree
Magnolia grandiflora (*Mg*)	Magnoliaceae	SE North America	Temperate humid	Evergreen	Tree
Quercus rubra (*Qr*)	Fagaceae	NE North America	Temperate	Deciduous	Tree
Vitis labrusca (*Vl*)	Vitaceae	E North America	Temperate	Deciduous	Vine

During the experimental period, trees received only natural precipitation (cumulative rainfall =243 mm). The mean temperature and relative humidity were 24.2 ± 1.9 °C and 75.3 ± 1%, respectively (weather station of Torre Faro, Messina, Italy).

Leaf water potential isotherms and measurements of leaf capacitance

Leaf water potential isotherms, also known as pressure–volume (PV) curves, were measured for five leaves per species to estimate leaf water potential at the turgor loss point (Ψ_{tlp}), osmotic potential at full turgor (π_0), bulk modulus of elasticity (ε_{max}), and leaf capacitance (C). Samples were cut under water and allowed to rehydrate for at least 1 h before generating PV curves using a pressure chamber to measure leaf water potential (Ψ_L) at regular intervals during progressive leaf dehydration. PV curves were elaborated to obtain Ψ_{tlp}, π_0, and ε_{max}. Leaf capacitance was also derived from PV curves on the basis of the slope of the relationship between water loss and Ψ_L both before ($C_{max,PV}$) and after Ψ_{tlp} ($C_{tlp,PV}$), and normalised by leaf area (A_L). At the end of each experiment, A_L was measured with a leaf area meter (Li3000A; Li-Cor Inc., Lincoln, NE, USA) and samples were dried in an oven for 3 d at 70 °C in order to measure leaf dry weight (DW).

Leaf hydraulic capacitance before and after turgor loss was also estimated during leaf rehydration (C_{FRT}) in order to compare values measured during the slow dehydration of the PV curve determination to values recorded during fast leaf rehydration (Blackman and Brodribb, 2011). C_{FRT} was estimated using the experimental procedure described by Nardini *et al.* (2012*b*). Ten leaves of each species were cut under water and allowed to rehydrate for 1 h. Leaves were then dehydrated on the bench to Ψ_L values corresponding to about 50% of species-specific Ψ_{tlp} (n=5), or down to Ψ_{tlp} (n=5). Leaves were then wrapped in plastic film, weighed to record their initial weight (W_0) and inserted in the pressure chamber in order to estimate the corresponding Ψ_L (Ψ_0). Once the balance pressure was reached, the cut section of the petiole was covered with deionised water and the pressure inside the chamber was released at a rate of 0.015 MPa s^{-1} down to atmospheric value, thus allowing leaf rehydration. At the end of pressure relaxation, excess water was adsorbed with a filter paper and the leaf was left inside the chamber for 5 min at atmospheric pressure to allow equilibration of water content and Ψ_L across all leaf tissues. Ψ_L was measured again (Ψ_f) and the sample was extracted from the chamber and weighed in order to obtain its final weight (W_f). Leaf capacitance in the turgor range ($C_{max,FRT}$) or at Ψ_{tlp} ($C_{tlp,FRT}$) was calculated as: $(W_f - W_0)/(\Psi_f - \Psi_0)$ and normalised by A_L.

Leaf hydraulic conductance and vulnerability

Leaf hydraulic conductance (K_{leaf}) at different dehydration levels was measured using both the rehydration kinetic method (RKM) (Brodribb and Holbrook, 2003) and the vacuum chamber method (VCM) (Nardini *et al.*, 2001). The experimental procedure allowed the values of K_{leaf} recorded with the two different techniques to be compared. Shoots were cut under water in the morning (between 07:30 h and 08:30 h) and rehydrated for at least 1 h to full turgor. Shoots were then bench-dehydrated until species-specific Ψ_{tlp} values were reached, and leaves were sampled at different dehydration levels to measure K_{leaf} with the two techniques (see details below). All K_{leaf} measurements were performed at normal laboratory irradiance (PPFD<10 µmol m^{-2} s^{-1}) and normalised at 20 °C.

Before each measurement, shoots were enclosed in a black plastic bag with a piece of wet filter paper inside for at least 30 min in order to stop transpiration and favour the equilibration of water potential values across all leaves. For RKM measurements, one leaf was sampled and used to measure initial water potential (Ψ_0). A second leaf adjacent to the first one was detached with the petiole immersed in 10 mM KCl solution filtered at 0.2 µm, and left to rehydrate for 30–90 s before measuring the final leaf water potential (Ψ_f). Leaf hydraulic conductance was then calculated as $K_{leaf} = C \times \ln(\Psi_0/\Psi_f)\ t^{-1}\ A_L^{-1}$, where C is the leaf capacitance (measured by the fast rehydration method, see above), t is the rehydration time, and A_L is leaf area measured at the end of the experiment (see above).

In the case of VCM measurements, leaves at different dehydration levels were cut under water and immediately connected via their petiole to rigid polyetheretherketone (PEEK) tubing that passed through the rubber seal of a 8.0-l PVC vacuum flask into a beaker containing 10 mM KCl solution. The beaker rested on a digital balance connected to a computer. Flow readings were recorded at 30-s intervals at pressures of –40, –20, and 0 kPa (with respect to the atmospheric value) induced in the flask by a vacuum pump. The flow (F) was plotted against the pressure applied (P) and K_{leaf} was calculated from the slope of the F-to-P linear relationship. K_{leaf} was then scaled by the leaf area, A_L, as recorded at the end of the experiment. Measurements were completed within 45–75 min maximum. We decided to avoid applying a vacuum below –40 kPa in order to avoid excessive cell rehydration during estimation of the partitioning of leaf hydraulic resistances (see below).

Leaves measured for K_{leaf} with VCM were also used to estimate the hydraulic resistance (R=1/K) of the leaf vascular (R_x, Scoffoni and Sack, 2015) and extra-vascular resistance (R_{ox}). After measuring K_{leaf} (K_{leaf}=1/R_{leaf}), the leaf was extracted from the vacuum chamber, minor veins (fourth order or higher) were severed with a scalpel (12–15 cuts cm^{-2}), and the hydraulic conductance of the leaf xylem (K_x=1/R_x) was measured using the VCM as described above. The hydraulic conductance of the extra-vascular pathway calculated as $R_{ox} = R_L - R_x$.

Values of K_{leaf} recorded during progressive leaf dehydration were plotted against the corresponding leaf water potential values, thus obtaining hydraulic vulnerability curves for each species with both methods. In addition, values of R_{leaf}, R_x, and R_{ox} were plotted against corresponding Ψ_L values in order to assess the relative contributions of the vascular and extra-vascular components to R_{leaf} changes during dehydration.

Morpho-anatomical traits

Leaf mass per unit area (LMA) was calculated as DW/A_L (where DW is leaf dry weight) on the same leaves used for PV analysis and K_{leaf} measurements by RKM. Leaf density was also calculated as the ratio between LMA and leaf thickness (see below). The eventual leaf shrinkage during progressive dehydration (Scoffoni *et al.*, 2014) was measured on at least ten leaves per species. Five shoots per species were cut under water in the morning, transported to the laboratory with their cut basal end immersed in the water, and were left for 1.5 h to promote full rehydration. Fully turgid leaves were collected and immediately measured for their fresh weight (FW), A_L, leaf thickness (T_L, estimated by averaging values recorded in the bottom, middle, and top thirds of the leaf with a digital calliper, accuracy ±0.01 mm), and leaf volume (V, estimated as $T_L \times A_L$). After full-turgor measurements, samples were fixed by their petiole to a bar opposite a fan to promote dehydration and were repeatedly measured for the above parameters at different Ψ_L values, until Ψ_{tlp} was reached. To estimate Ψ_L, 15 leaves (different from those utilized to measure leaf shrinkage) were collected and randomly put next to leaves used for shrinkage measurements. Two leaves for each level of dehydration were randomly selected to estimate Ψ_L with a pressure chamber.

Because *A. moluccana* and *M. grandiflora* leaves curled at low Ψ_L, we were not able to estimate A_L and V during dehydration for these species. In *M. grandiflora*, percentage loss of leaf area was measured for ten leaves that had been weighed at full turgor and then cut into pieces before drying in the oven to avoid leaf curling (Scoffoni *et al.*, 2014). Unfortunately, this procedure was not adequate to estimate leaf area of dried samples of *A. moluccana* because the dried leaf pieces were also curled. Leaves measured for shrinkage during dehydration as well as samples measured for leaf water potential isotherms were also used to calculate leaf dry matter content (LDMC), as DW/FW.

In order to estimate vein density (VD), eight leaves per species were cut into 10 × 10 mm samples and maintained in 1M KOH for 5–8 d. Samples were repeatedly washed with water, immersed in 0.5% toluidine blue for 1 min, and washed again. Leaf images were acquired with a scanner (HP Scanjet G4050, USA) and analysed using the software ImageJ (http://imagej.nih.gov/ij/). Vein density (VD) was expressed as vein length per unit leaf area (mm mm^{-2}).

Statistical analysis

Data were analysed with the software SigmaStat v. 2.0 (SPSS, Inc., Chicago, IL, USA) and R v. 3.2.2 (www.r-project.org). The significance of differences among species was tested using one-way-ANOVA followed by Tukeys's *post hoc* comparisons. Differences in capacitance values recorded by PV analysis and by the fast rehydration method were tested with Student's *t*-test. A correlation matrix of all measured parameters was performed (see Supplementary Table S3 at *JXB* online). The significance of correlations was tested using the Pearson product-moment coefficient. An ANCOVA was used to test for statistical significance of differences between species in terms of responses of R_{leaf}, R_x and R_{ox}, to Ψ_L (Supplementary Tables S1 and S2). All regressions or differences were considered significant at $P<0.05$.

Results

Values of Ψ_{tlp} ranged between –1.6 MPa in *V. labrusca* and –3.1 MPa in *Q. rubra*. The same trend was recorded for π_0, which averaged –1.3 and –2.4 MPa in *V. labrusca* and *Q. rubra*, respectively (Table 2). *Aleurites moluccana* and *M. grandiflora* displayed similar Ψ_{tlp} (about –2.3 MPa) but slightly different values of π_0 (–1.9 and –1.6 MPa, respectively). The bulk modulus of elasticity at full turgor ranged from 11 MPa in *V. labrusca* to about 23 MPa in *A. moluccana*.

No statistically significant differences were recorded between leaf capacitance values measured on the basis of PV curves or by fast rehydration in *A. moluccana* and in *M. grandiflora*, either before or after the turgor-loss point (Table 3). In contrast, in *Q. rubra* and in *V. labrusca*, C_{max} and C_{tlp} values recorded from PV analysis were significantly higher than values recorded by fast rehydration. In particular, C_{max} was 418 mmol m^{-2} MPa^{-1} in *Q. rubra* and 726 mmol m^{-2} MPa^{-1} in *V. labrusca* when measured on the basis of PV curves, but only 205 mmol m^{-2} MPa^{-1} and 100 mmol m^{-2} MPa^{-1}, respectively, when measured during fast rehydration. Similar differences were observed for C_{tlp} (Table 3). Blackman and Brodribb (2010) have suggested that when differences in leaf capacitance are observed between different techniques, values measured by the fast rehydration method should be preferred as they assure a more accurate estimation of K_{leaf}. Therefore, we decided to use values of leaf capacitance that were estimated by the rehydration kinetic method for estimating K_{leaf} in all cases in this study.

Maximum values of K_{leaf} measured using VCM were similar to those obtained on the basis of RKM in all species except *Q. rubra* (Fig. 1). For this species, maximum values of K_{leaf} of about 11 mmol m^{-2} s^{-1} MPa^{-1} were recorded with RKM, versus about 5.4 mmol m^{-2} s^{-1} MPa^{-1} recorded with VCM. Despite this difference, the two methods produced

Table 2. *Leaf water potential at turgor loss point (Ψ_{tlp}), osmotic potential at full turgor (π_0) and bulk modulus of elasticity (ε_{max}) as recorded by pressure–volume analysis in the species under study. For each parameter, different letters indicate statistically significant differences between species. Means are reported ±SD*

	Am	*Mg*	*Qr*	*Vl*
$-\Psi_{tlp}$ (MPa)	2.5 ± 0.1a	2.2 ± 0.3a	3.1 ± 0.14b	1.6 ± 0.06c
$-\pi_0$ (MPa)	1.9 ± 0.12a	1.6 ± 0.13b	2.4 ± 0.11c	1.3 ± 0.04d
ε_{max} (MPa)	23 ± 3.8a	14 ± 3.0b	21 ± 2.9a	11 ± 1.2b

Table 3. *Leaf capacitance at full turgor and at the turgor-loss point as recorded by pressure–volume analysis ($C_{max,PV}$ and $C_{tlp,PV}$, respectively) and by fast leaf rehydration ($C_{max,FRT}$ and $C_{tlp,FRT}$) in the species under study. Values of leaf capacitance are normalized by leaf area. Different letters indicate statistically significant differences. Means are reported ±SD*

Species	$C_{max,PV}$	$C_{max,\ FRT}$	$C_{tlp,\ PV}$	$C_{tlp,FRT}$
	mmol MPa^{-1}m^{-2}		mmol MPa^{-1}m^{-2}	
Am	456 ± 55a	456 ± 88a	951 ± 180a	950 ± 110a
Mg	229 ± 17a	275 ± 80a	326 ± 90b	325 ± 85b
Qr	418 ± 30a	205 ± 7.8b	1360 ± 280a	972 ± 1.7b
Vl	726 ± 44a	100 ± 20b	2382 ± 468a	380 ± 90b

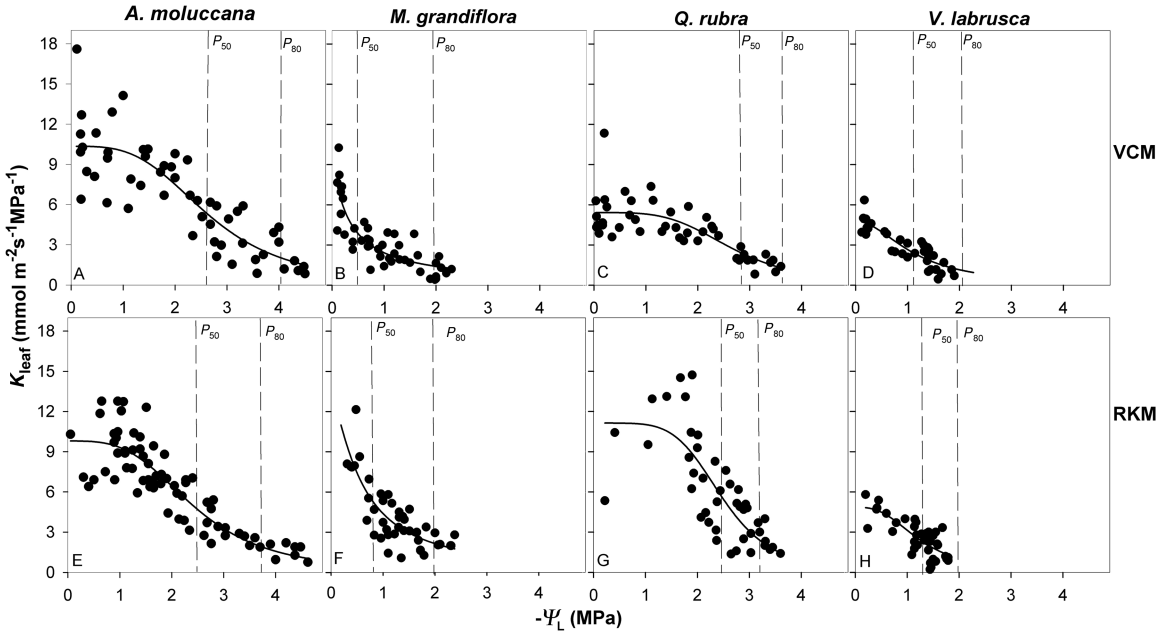

	K_{max} (mmol m^{-2} s^{-1} MPa^{-1})		P_{50} (MPa)		P_{80} (MPa)	
	VCM	RKM	VCM	RKM	VCM	RKM
Am	10.3	9.8	-2.68	-2.45	-4.05	-3.75
Mg	10.1	11.1	-0.45	-0.80	-1.95	-2.05
Qr	5.4	11.1	-2.83	-2.45	-3.65	-3.23
Vl	4.8	4.9	-1.15	-1.30	-2.10	-2.03

Fig. 1. Relationships between leaf hydraulic conductance (K_{leaf}) and leaf water potential (Ψ_L) as recorded in the study species using the vacuum chamber method (VCM) or the rehydration kinetics method (RKM). Curves were fitted to the data with three-parameter logistic functions: $y = a/[1 + (x/x_0)^b]$. Dashed lines indicate the leaf water potential values inducing 50% (P_{50}) and 80% (P_{80}) loss of K_{leaf}. Maximum values of leaf hydraulic conductance (K_{max}), P_{50} and P_{80} obtained with the two techniques are shown in the table below the figure. See Table 1 for abbreviations of species' names.

similar trends of K_{leaf} changes during progressive dehydration. Accordingly, leaf water potential values inducing 50% (P_{50}) or 80% (P_{80}) loss of K_{leaf} were similar when calculated on the basis of VCM or RKM measurements, with differences between the techniques always <0.4 MPa. The highest (less negative) P_{50} and P_{80} values were recorded in *M. grandiflora* (about –0.6 and –2 MPa, respectively). In *V. labrusca*, P_{50} and P_{80} were about –1.2 and –2.0 MPa, respectively. *Aleurites moluccana* and *Q. rubra* showed quite similar values of P_{50} (about –2.5 MPa and –2.6 MPa, respectively), but P_{80} was lower in *A. moluccana* than in *Q. rubra* (about –3.9 MPa versus about –3.5 MPa, respectively).

Figure 2 shows changes of R_{leaf}, R_x, and R_{ox} as a function of Ψ_L during progressive leaf dehydration. In *A. moluccana* and *V. labrusca*, R_{leaf}, R_x, and R_{ox} changed in response to Ψ_L following a similar trend. By contrast, in *M. grandiflora* and *Q. rubra* values of R_{ox} increased during progressive dehydration in parallel with changes of R_{leaf}, while R_x remained substantially invariant (Supplementary Table S1). When relative values of whole-leaf hydraulic resistance were plotted against relative values of both vascular and extra-vascular hydraulic resistances (Fig. 3), significant linear correlations emerged. However, in *A. moluccana* and *V. labrusca* the slopes of R_{leaf} versus R_x or R_{ox} were remarkably similar (and not significantly different in the case of *V. labrusca*), indicating co-limitation of R_{leaf} by R_x and R_{ox}. In *M. grandiflora* and *Q. rubra* the slopes of the relationships were largely and significantly different (Supplementary Table S2). In particular, relative changes of R_{leaf} were more markedly influenced by relative changes of R_{ox} than by R_x in both species.

LMA ranged between 45 g m^{-2} (*V. labrusca*) and 212 g m^{-2} (*M. grandiflora*, Table 4), while leaf density was lowest in *V. labrusca* (0.22 g cm^{-3}) and highest in *Q. rubra* (0.41 g cm^{-3}). Leaf thickness at full turgor was around 0.20 mm in *Q. rubra* and *V. labrusca*, with higher values in *A. moluccana* (0.37 mm) and *M. grandiflora* (0.73 mm). At the turgor-loss point, leaf thickness decreased by about 25% in *A. moluccana*, *M. grandiflora*, and *Q. rubra*, and by about 33% in *V. labrusca*. The percentage decrease of leaf thickness of a dry leaf compared to full turgor was about 42% in *A. moluccana*, *M. grandiflora*, and *Q. rubra*, and about 55% in *V. labrusca*, which also showed the highest percentage decrease of leaf area (about 37%) and leaf volume (about 57%). Vein density was about 5.8 mm mm^{-2} in *A. moluccana* and *M. grandiflora*, and about 6.9 mm mm^{-2} in *Q. rubra* and *V. labrusca*. LDMC ranged between 250 mg g^{-1} (*V. labrusca*) and about 418 mg g^{-1} (*M. grandiflora* and *Q. rubra*). Leaf hydraulic resistance values measured during progressive dehydration were well correlated with leaf thickness in *M. grandiflora* and *Q. rubra*, but only weakly in *A. moluccana* and *V. labrusca* (Fig. 4).

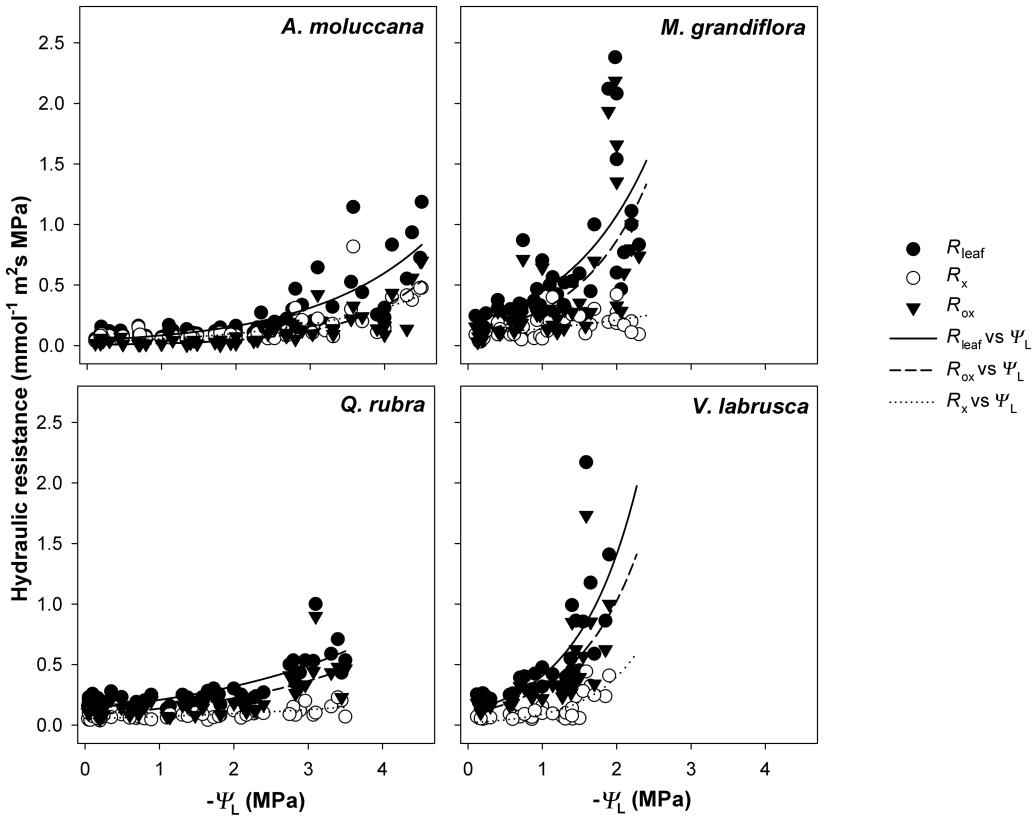

Fig. 2. Hydraulic resistance of whole leaf (R_{leaf}, black circles, solid line), vascular pathway (R_x, white circles, dotted line), and extra-vascular pathway (R_{ox}, black inverted triangles, dashed line) as a function of leaf water potential (Ψ_L) as recorded in the study species. Regression curves were expressed by the following function: $y = ae^{bx}$.

The slope of the change in leaf thickness down to $\Psi_L = -0.5$ MPa was linearly correlated to P_{80} and ε_{max} across the four study species, but only weakly correlated to leaf density (Fig. 5). Moreover, leaf density (but not ε_{max}) was correlated with several indicators of leaf shrinkage (i.e. leaf thickness at the turgor-loss point, the ratio of leaf thickness values and leaf water potential values up to the turgor-loss point, and the percentage loss of leaf thickness for a dry leaf, Supplementary Table S3). By contrast, ε_{max} was linearly correlated with leaf hydraulic vulnerability, although the correlation with P_{50} was weak (Fig. 6).

Discussion

Parallel measurements of R_x and R_{ox} during leaf dehydration revealed that the relative contribution of vascular and extra-vascular hydraulic properties in driving K_{leaf} decline during dehydration is species-specific. While in *A. moluccana* and *V. labrusca* the progressive impairment of both vascular and extra-vascular pathways contributed to leaf hydraulic vulnerability, in the other two study species (*M. grandiflora* and *Q. rubra*) the vascular pathway remained substantially unaltered during leaf dehydration, and K_{leaf} decline was apparently caused only by changes in the hydraulic properties of the extra-vascular compartment.

The species selected covered a wide range of capacitance, LMA, and Ψ_{tlp} values, reflecting a spectrum of drought tolerance levels (Ishida *et al.*, 2008; Bartlett *et al.*, 2012). This was confirmed by the analysis of leaf hydraulic vulnerability, with P_{50} values ranging from –0.45 MPa to –2.83 MPa, a range very similar to the global spectrum of P_{50} values recently reported in a meta-analysis by Nardini and Luglio (2014).

Interestingly, the two hydraulic techniques based on vacuum pressure or rehydration kinetics yielded very similar results in terms of maximum K_{leaf} values (recorded at near-full turgor) as well as in terms of progressive K_{leaf} decline during dehydration, as revealed by similar P_{50} and P_{80} values derived from vulnerability curves assessed with VCM or RKM (Fig. 1). While the consistency of different hydraulic techniques for measuring maximum K_{leaf} has been previously reported for different assemblages of species (Sack *et al.*, 2002; Nardini *et al.*, 2010; Flexas *et al.*, 2013), only one recent study has provided comparisons of different methods to assess K_{leaf} responses to declining Ψ_L (Hernandez-Santana *et al.*, 2016). Our data suggest that both VCM and RKM can be used for this purpose, and the agreement between the two methods supports the robustness of the results obtained, tending to validate P_{50} or P_{80} values obtained in this and other studies using these procedures.

It must be noted that agreement between VCM and RKM was observed in this study when K_{leaf} values based on RKM were calculated using leaf capacitance values measured using a fast rehydration method, and not those derived from PV curve analysis, which were significantly higher in two out of the four species (*Q. rubra* and *V. labrusca*, Table 3). These findings are in agreement with Blackman

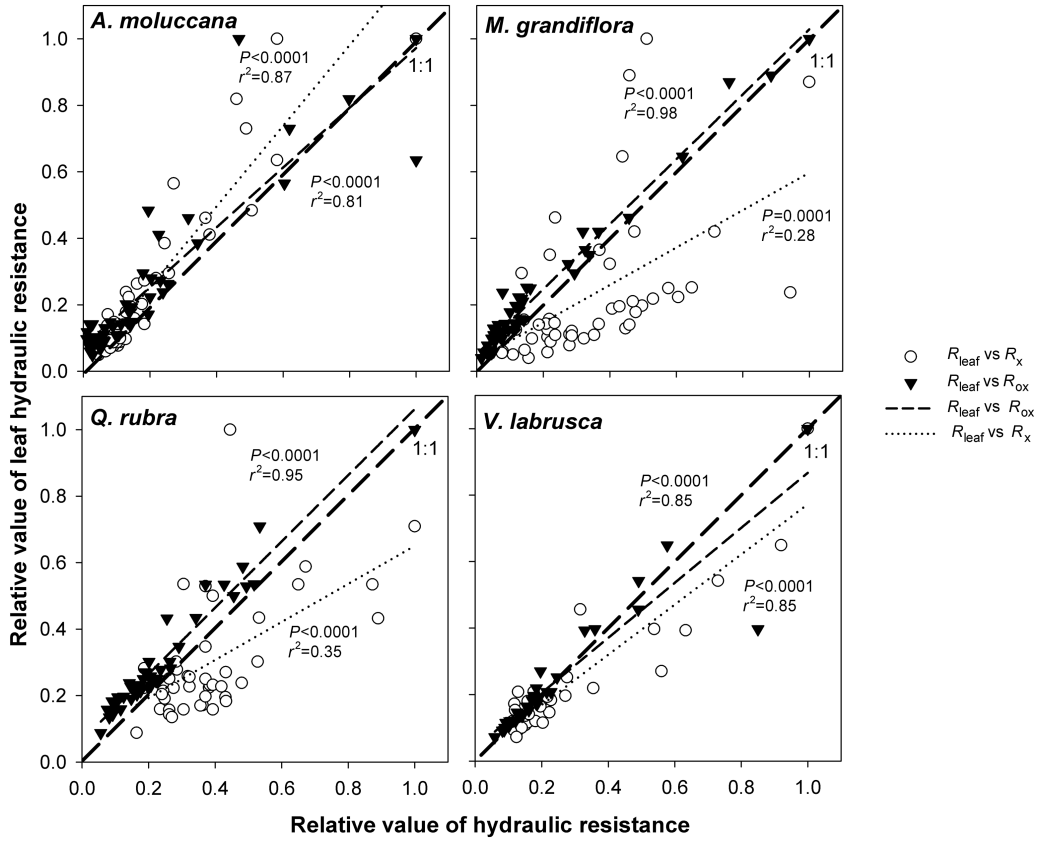

Fig. 3. Relationships between relative value of whole-leaf hydraulic resistance (R_{leaf}) and the relative values of vascular hydraulic resistance (R_x, white circles, dotted line) and extra-vascular hydraulic resistance (R_{ox}, black inverted triangles, dashed line) as recorded in the study species. Regression lines are expressed by the following function: $y = y_0 + ax$. Values of correlation coefficients (r^2) and *P*-values are indicated for each curve. The thick dashed lines indicate the 1:1 relationship.

Table 4. *Leaf area (A_L), leaf mass per area (LMA), leaf dry matter content (LDMC), leaf volume (V), leaf density, leaf thickness at full turgor (T_L) and at the turgor-loss point ($T_{L,\,tlp}$), percentage loss of leaf thickness (PLT_{dry}), leaf area (PLA_{dry}) and leaf volume (PLV_{dry}) of a dry leaf, and leaf vein density (VD) as recorded in the study species. Means are given ±SD (*n = 53, 47, 46, 15 and 35 for A_L, LMA, LDMC and leaf density; n=10 for V, T_L, $T_{L,tlp}$, PLT_{dry}, PLA_{dry}, PLV_{dry}; n = 8 for VD). Different letters indicate statistically significant differences between species*

	Am	*Mg*	*Qr*	*Vl*
A_L (cm^2)	17.6±3.4a	9.4±2b	8.3±1.7b	13.8±3.1c
LMA ($g\ m^{-2}$)	118.7±13a	212±20b	83±12c	45±11d
LDMC ($mg\ g^{-1}$)	323±16a	418±20b	412±12b	250±25c
V (cm^3)	6.5±1.4a	6.4±1a	1.6±0.4b	2.7±0.3c
Leaf density ($g\ cm^{-3}$)	0.33±0.08a	0.34±0.03ab	0.41±0.09b	0.22±0.02c
T_L (mm)	0.37±0.05a	0.73±0.07b	0.19±0.03c	0.20±0.03c
$T_{L,\,tlp}$ (mm)	0.28±0.03a (25±4%)	0.55±0.05b (25±3%)	0.15±0.02c (23±4%)	0.14±0.01c (33±3%)
PLT_{dry} (%)	44±8a	42±7a	40±6a	55±4b
PLA_{dry} (%)	–	11.7±3.7a	13.7±3.5a	37±3.6b
PLV_{dry} (%)	–	28±4a	37±6b	57±6c
VD ($mm\ mm^{-2}$)	5.6±0.8a	5.9±0.4a	6.9±0.4b	6.9±0.9b

and Brodribb (2011), and suggest that caution must be adopted with regards to the accuracy of measuring leaf capacitance during rehydration when K_{leaf} is evaluated using RKM. Moreover, higher values of leaf capacitance measured during slow dehydration than under fast rehydration strongly suggest that in some species leaf tissues are hydraulically compartmentalized, and probably are not involved to the same extent in water transport across the leaf (Nardini *et al.*, 2010; Canny *et al.*, 2012).

The VCM allowed the separation of the effects of R_x and R_{ox} on the overall change of R_{leaf} during progressive dehydration. It must be noted that the procedure may be prone to errors, as partial leaf rehydration occurs during the initial R_L measurement. This is not expected to impact on R_x

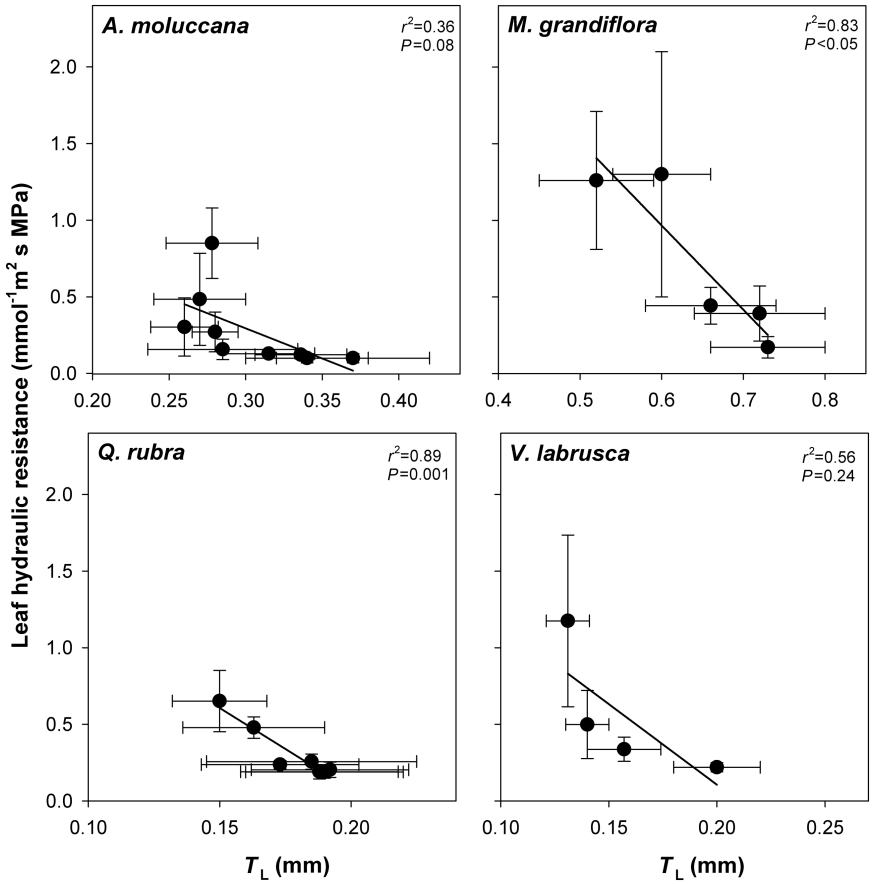

Fig. 4. Mean values (±SD) of leaf hydraulic resistance versus leaf thickness (T_L) as recorded at 0.5 MPa intervals during dehydration in leaves of the study species. Regression curves are expressed by the following function: $y = y_0 + ax$. Correlation coefficients (r^2) and P-values are indicated.

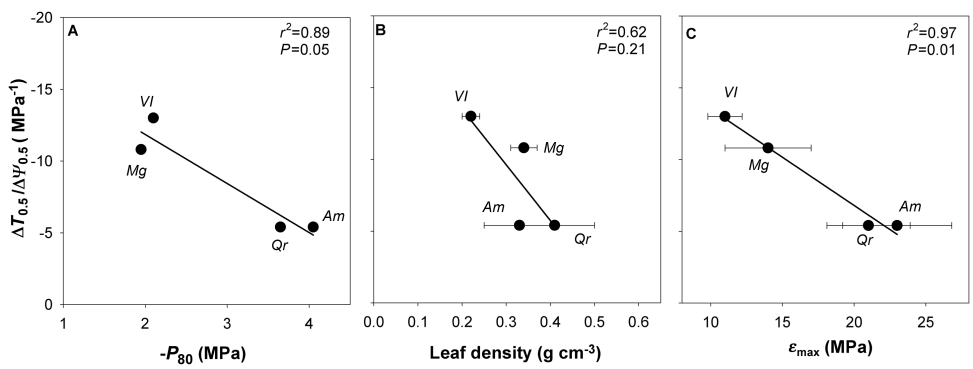

Fig. 5. Relationships between the slope of leaf shrinkage at Ψ_L = –0.5 MPa ($\Delta T_{0.5}/\Delta\Psi_{0.5}$) and (A) leaf water potential inducing 80% loss of hydraulic conductance (P_{80}), (B) leaf density (mean values ±SD), and (C) bulk modulus of elasticity (ε_{max}, mean values ±SD) as recorded in the species under study. Regression curves are expressed by the following function: $y = y_0 + ax$. Values of correlation coefficients (r^2) and P-values are indicated. See Table 1 for abbreviations of species' names.

values, as vein refilling has not been observed during VCM experiments over the time interval typically required to complete hydraulic measurements on a single leaf (Nardini *et al.*, 2003). However, partial cell rehydration might have an impact on R_{ox}, to an extent that cannot be predicted on the basis of our data. Moreover, it must be noted that our measurements were performed under low irradiance (PPFD <10 µmol m^{-2} s^{-1}). Therefore, it cannot be ruled out that different trends of R_x and R_{ox} in response to dehydration may occur in species whose leaf hydraulic conductance changes in response to irradiance. Hence, while our experiments represent an attempt to actually measure R_x and R_{ox} during leaf dehydration, the interpretation of R_{ox} values obtained with the VCM method should be cautious.

During dehydration of *A. moluccana* and *V. lab*rusca leaves, both R_x and R_{ox} increased in parallel with increasing R_{leaf}. This pattern would suggest progressive impairment of both vascular and extra-vascular pathways under water stress in these species, as also revealed by plotting relative R_{leaf} values against relative R_x and R_{ox} (Fig. 3). The increase in R_x was

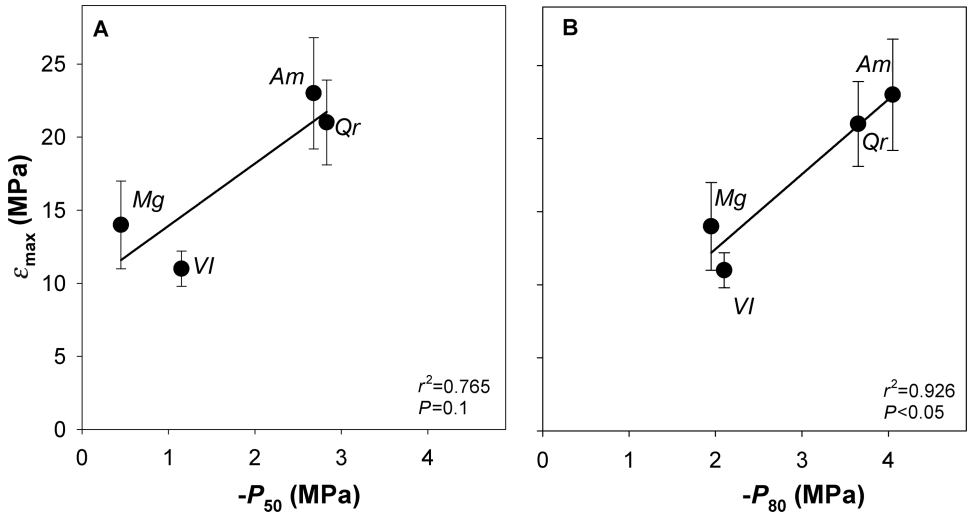

Fig. 6. Relationships between the bulk modulus of elasticity (ε_{max}) and the leaf water potential inducing (A) 50% (P_{50}) or (B) 80% (P_{80}) loss of leaf hydraulic conductance. Regression curves are expressed by the following function: $y = y_0 + ax$. Values of correlation coefficients (r^2) and P-values are indicated. See Table 1 for abbreviations of species' names.

probably due to vein embolism formation, a factor that has been previously reported as a major driver of leaf hydraulic impairment under drought (Salleo *et al.*, 2001; Nardini *et al.*, 2003; Johnson *et al.*, 2009*a*; Brodribb *et al.*, 2016). However, our data reveal that the R_{leaf} increase was only partially explained by vascular hydraulic failure, and a significant contribution to leaf hydraulic vulnerability was due to changes in the hydraulic properties of the extra-vascular pathway. This was much more apparent in the other two species investigated (*M. grandiflora* and *Q. rubra*), where R_x remained substantially invariant during leaf dehydration, and changes in R_{leaf} were mostly due to an increase in R_{ox}. These findings would suggest that in these species vein xylem is quite resistant to embolism formation, but nevertheless K_{leaf} declines during dehydration because of modifications of the extra-vascular water pathway.

In accordance with the above conclusion, R_{leaf} was significantly correlated to leaf thickness in *M. grandiflora* and *Q. rubra*, but not in *A. moluccana* and *V. labrusca* (Fig. 4), suggesting a relationship between changes in leaf thickness and R_{ox} during dehydration. In turn, leaf shrinkage was significantly correlated to ε_{max} and P_{80}, and weakly associated to leaf density (Fig. 5). Overall, these findings suggest that changes in R_{ox} are at least partly caused by progressive shrinkage of mesophyll cells, which would be more likely in species with thinner and more elastic cell walls, as suggested by lower ε_{max}. Nevertheless, it cannot be ruled out that shrinkage of mesophyll cells is a consequence of shrinkage of other cell types, such as those located at the bundle sheath. Our results confirm previous findings by Scoffoni *et al.* (2014) indicating that changes in cell shape and connectivity under drought may lead to increased R_{ox} with significant impacts on R_{leaf}, and possibly on gas exchange, even if the vein xylem does not experience significant embolism levels. It might be also hypothesised that in some species the hydraulic vulnerability of the extra-vascular pathway acts as a 'hydraulic signal' to increase R_{leaf} and induce stomatal closure before leaf water potential and vein xylem pressure drop to critical values triggering xylem embolism (Rockwell *et al.*, 2014; Scoffoni *et al.*, 2014; Bouche *et al.*, 2016). In a way, this scenario would resemble the role of high leaf hydraulic vulnerability as a protective mechanism to maintain stem hydraulic efficiency even under severe drought, which has been recognised as an important adaptation of plants growing in drought-prone habitats (Pivovaroff *et al.*, 2014; Zhu *et al.*, 2016). In other words, the hypothesis that vulnerability segmentation plays a role in protecting the integrity of the plant hydraulic system (Tyree *et al.*, 1993; Choat *et al.*, 2005; Savi *et al.*, 2016) would stand at both inter- and intra-organ levels.

A protective mechanism of the leaf vascular system based on R_{ox} increasing under water stress as a consequence of cell shrinkage would also probably guarantee short-term reversibility of K_{leaf} decline upon leaf rehydration, providing an alternative or additional explanation for previous reports of fast post-drought recovery of leaf hydraulic properties in different species (Trifilò *et al.*, 2003*a*; Scoffoni *et al.*, 2012; Savi *et al.*, 2016), which were in some cases attributed to embolism repair in vein xylem conduits.

The correlation of ε_{max} with leaf hydraulic vulnerability (Fig. 6) is in agreement with a previous report by Blackman *et al.* (2010) and offers a possible new mechanistic interpretation for this functional trait. In fact, high values of ε_{max} translated into reduced leaf shrinkage and more negative P_{50} and P_{80} values. Species adapted or acclimated to dry habitats have often been reported to have higher ε_{max}, indicating thicker and/or stiffer cell walls (Abrams *et al.*, 1990; Chimenti and Hall, 1994). In these cases, the increase in ε_{max} might be interpreted as a mechanism to decrease leaf hydraulic vulnerability, thus improving the capacity to maintain leaf hydraulic efficiency and gas exchange rates even under conditions of reduced soil water availability and/or high atmospheric evaporative demand.

In conclusion, our data provide support for species-specific patterns of R_x and R_{ox} changes during leaf dehydration, and

their consequent impacts on leaf hydraulic efficiency. The possible protective role of the vulnerability of the extra-vascular water pathway with regards to embolism formation in the vein xylem deserves additional studies on larger species' assemblages, to disentangle the eventual adaptive role of this mechanism in different habitats with contrasting levels of water availability and drought frequency/intensity.

Supplementary data

Table S1. Summary of ANCOVA analyses and results of pairwise differences using Tukey's *post hoc* test for the responses of leaf hydraulic resistance, xylem hydraulic resistance, and leaf outside-xylem resistance to declining leaf water potential in the four study species.

Table S2. Summary of ANCOVA analyses for the response of relative values of xylem hydraulic resistance and leaf outside-xylem resistance to increasing relative values of the whole-leaf hydraulic resistance in the four study species.

Table S3. Correlation matrix of 28 measured leaf traits across the four study species.

References

Abrams MD, Kubiske ME, Steiner KC. 1990. Drought adaptations and responses in five genotypes of *Fraxinus pennsylvanica* Marsh.: photosynthesis, water relations and leaf morphology. Tree Physiology **6,** 305–315.

Bartlett MK, Scoffoni C, Sack L. 2012. The determinants of leaf turgor loss point and prediction of drought tolerance of species and biomes: a global meta-analysis. Ecology Letters **15,** 393–405.

Blackman CJ, Brodribb TJ. 2011. Two measures of leaf capacitance: insights into the water transport pathway and hydraulic conductance in leaves. Functional Plant Biology **38,** 118–126.

Blackman CJ, Brodribb TJ, Jordan GJ. 2010. Leaf hydraulic vulnerability is related to conduit dimensions and drought resistance across a diverse range of woody angiosperms. New Phytologist **188,** 1113–1123.

Bouche PS, Delzon S, Choat B, *et al.* 2016. Are needles of *Pinus pinaster* more vulnerable to xylem embolism than branches? New insights from X-ray computed tomography. Plant, Cell and Environment **39,** 860–870.

Brodribb TJ, Holbrook NM. 2003. Stomatal closure during leaf dehydration, correlation with other leaf physiological traits. Plant Physiology **132,** 2166–2173.

Brodribb TJ, Holbrook NM. 2006. Declining hydraulic efficiency as transpiring leaves desiccate: two types of response. Plant, Cell and Environment **29,** 2205–2215.

Brodribb TJ, Holbrook NM, Zwieniecki MA, Palma B. 2005. Leaf hydraulic capacity in ferns, conifers and angiosperms: impacts on photosynthetic maxima. New Phytologist **165,** 839–846.

Brodribb TJ, Skelton RP, McAdam SAM, Bienaimé D, Lucani CJ, Marmottant P. 2016. Visual quantification of embolism reveals leaf vulnerability to hydraulic failure. New Phytologist **209,** 1403–1409.

Buckley TN. 2015. The contributions of apoplastic, symplastic and gas phase pathways for water transport outside the bundle sheath in leaves. Plant, Cell and Environment **38,** 7–22.

Buckley TN, Grace PJ, Scoffoni C, Sack L. 2015. How does leaf anatomy influence water transport outside the xylem? Plant Physiology **168,** 1616–1635.

Canny M, Wong SC, Huang C, Miller C. 2012. Differential shrinkage of mesophyll cells in transpiring cotton leaves: implications for static and dynamic pools of water, and for water transport pathways. Functional Plant Biology **39,** 91–102.

Charra-Vaskou K, Badel E, Burlett R, Cochard H, Delzon S, Mayr S. 2012. Hydraulic efficiency and safety of vascular and non-vascular components in *Pinus pinaster* leaves. Tree Physiology **32,** 1161–1170.

Chimenti CA, Hall AJ. 1994. Responses to water stress of apoplastic water fraction and bulk modulus of elasticity in sunflower (*Helianthus annuus* L.) genotypes of contrasting capacity for osmotic adjustment. Plant and Soil **166,** 101–107.

Choat B, Lahr EC, Melcher PJ, Zwieniecki MA, Holbrook NM. 2005. The spatial pattern of air seeding thresholds in mature sugar maple trees. Plant, Cell and Environment **28,** 1082–1089.

Cochard H, Nardini A, Coll L. 2004. Hydraulic architecture of leaf blades: where is the main resistance? Plant, Cell and Environment **27,** 1257–1267.

Flexas J, Scoffoni C, Gago J, Sack L. 2013. Leaf mesophyll conductance and leaf hydraulic conductance: an introduction to their measurement and coordination. Journal of Experimental Botany **64,** 3965–3981.

Gascó A, Nardini A, Salleo S. 2004. Resistance to water flow through leaves of *Coffea arabica* is dominated by extra-vascular tissues. Functional Plant Biology **31,** 1161–1168.

Heinen RB, Ye Q, Chaumont F. 2009. Role of aquaporins in leaf physiology. Journal of Experimental Botany **60,** 2971–2985.

Hernandez-Santana V, Rodriguez-Dominguez CM, Fernandez JE, Diaz-Espejo A. 2016. Role of leaf hydraulic conductance in the regulation of stomatal conductance in almond and olive in response to water stress. Tree Physiology **36,** 725–735.

Ishida A, Nakano T, Yazaki K, Matsuki S, Koike N, Lauenstein DL, Shimizu M, Yamashita N. 2008. Coordination between leaf and stem traits related to leaf carbon gain and hydraulics across 32 drought-tolerant angiosperms. Oecologia **156,** 193–202.

Johnson DM, Meinzer FC, Woodruff DR, McCulloh KA. 2009*a*. Leaf xylem embolism, detected acoustically and by cryo-SEM, corresponds to decreases in leaf hydraulic conductance in four evergreen species. Plant, Cell and Environment **32,** 828–836.

Johnson DM, Woodruff DR, McCulloh KA, Meinzer FC. 2009*b*. Leaf hydraulic conductance, measured *in situ*, declines and recovers daily: leaf hydraulics, water potential and stomatal conductance in four temperate and three tropical species. Tree Physiology **29,** 879–887.

Kikuta SB, Lo Gullo MA, Nardini A, Richter H, Salleo S. 1997. Ultrasound acoustic emissions from dehydrating leaves of deciduous and evergreen trees. Plant, Cell and Environment **20,** 1381–1390.

Kim YX, Steudle E. 2007. Light and turgor affect the water permeability (aquaporins) of parenchyma cells in the midrib of leaves of *Zea mays*. Journal of Experimental Botany **58,** 4119–4129.

Laur J, Hacke UG. 2014. The role of water channel proteins in facilitating recovery of leaf hydraulic conductance from water stress in *Populus trichocarpa*. PLoS ONE **9,** e111751.

Lo Gullo MA, Nardini A, Trifilò P, Salleo S. 2003. Changes in leaf hydraulics and stomatal conductance following drought stress and irrigation in *Ceratonia siliqua* (Carob tree). Physiologia Plantarum **117,** 186–194.

Martorell S, Medrano H, Tomàs M, Escalona JM, Flexas J, Diaz-Espejo A. 2015. Plasticity of vulnerability to leaf hydraulic dysfunction during acclimation to drought in grapevines: an osmotic-mediated process. Physiologia Plantarum **153,** 381–391.

Miniussi M, Del Terra L, Savi T, Pallavicini A, Nardini A. 2015. Aquaporins in *Coffea arabica* L.: identification, expression, and impacts on plant water relations and hydraulics. Plant Physiology and Biochemistry **95,** 92–102.

Nardini A, Luglio J. 2014. Leaf hydraulic capacity and drought vulnerability: possible trade-offs and correlations with climate across three major biomes. Functional Ecology **28,** 810–818.

Nardini A, Pedà G, La Rocca N. 2012*a*. Trade-offs between leaf hydraulic capacity and drought vulnerability: morpho-anatomical bases, carbon costs and ecological consequences. New Phytologist **196,** 788–798.

Nardini A, Pedà G, Salleo S. 2012*b*. Alternative methods for scaling leaf hydraulic conductance offer new insights into the structure-function relationships of sun and shade leaves. Functional Plant Biology **39,** 394–401.

Nardini A, Raimondo F, Lo Gullo MA, Salleo S. 2010. Leafminers help us understanding leaf hydraulic design. Plant, Cell and Environment **33,** 1091–1100.

Nardini A, Ramani M, Gortan E, Salleo S. 2008. Vein recovery from embolism occurs under negative pressure in leaves of sunflower (*Helianthus annuus*). Physiologia Plantarum **133,** 755–764.

Nardini A, Salleo S. 2003. Effects of the experimental blockage of the major veins on hydraulics and gas exchange of *Prunus laurocerasus* L. leaves. Journal of Experimental Botany **54,** 1213–1219.

Nardini A, Salleo S, Andri S. 2005. Circadian regulation of leaf hydraulic conductance in sunflower (*Helianthus annuus* L. cv Margot). Plant, Cell and Environment **28,** 750–759.

Nardini A, Salleo S, Raimondo F. 2003. Changes in leaf hydraulic conductance correlate with leaf vein embolism in *Cercis siliquastrum* L. Trees **17,** 529–534.

Nardini A, Tyree MT, Salleo S. 2001. Xylem cavitation in the leaf of *Prunus laurocerasus* and its impact on leaf hydraulics. Plant Physiology **125,** 1700–1709.

Pivovaroff AL, Sack L, Santiago LS. 2014. Coordination of stem and leaf hydraulic conductance in southern California shrubs: a test of the hydraulic segmentation hypothesis. New Phytologist **203,** 842–850.

Rockwell FE, Holbrook NM, Stroock AD. 2014. The competition between liquid and vapor transport in transpiring leaves. Plant Physiology **164,** 1741–1758.

Ryu J, Hwang BG, Kim YX, Lee SJ. 2016. Direct observation of local xylem embolisms induced by soil drying in intact *Zea mays* leaves. Journal of Experimental Botany **67,** 2617–2626.

Sack L, Dietrich EM, Streeter CM, Sánchez-Gómez D, Holbrook NM. 2008. Leaf palmate venation and vascular redundancy confer tolerance of hydraulic dysfunction. Proceedings of the National Academy of Sciences USA **105,** 1567–1572.

Sack L, Holbrook NM. 2006. Leaf hydraulics. Annual Review of Plant Biology **57,** 361–381.

Sack L, Melcher PJ, Zwieniecki MA, Holbrook NM. 2002. The hydraulic conductance of the angiosperm leaf lamina: a comparison of three measurement methods. Journal of Experimental Botany **53,** 2177–2184.

Sack L, Scoffoni C. 2013. Leaf venation: structure, function, development, evolution, ecology and applications in the past, present and future. New Phytologist **198,** 983–1000.

Sack L, Tyree MT, Holbrook NM. 2005. Leaf hydraulic architecture correlates with regeneration irradiance in tropical rainforest trees. New Phytologist **167,** 403–413.

Salleo S, Lo Gullo MA, Raimondo F, Nardini A. 2001. Vulnerability to cavitation of leaf minor veins: any impact on leaf gas exchange? Plant, Cell and Environment **24,** 851–859.

Salleo S, Raimondo F, Trifilò P, Nardini A. 2003. Axial-to-radial water permeability of leaf major veins: a possible determinant of the impact of vein embolism on leaf hydraulics? Plant, Cell and Environment **26,** 1749–1758.

Santiago LS, Goldstein G, Meinzer FC, Fisher JB, Machado K, Woodruff D, Jones T. 2004. Leaf photosynthetic traits scale with hydraulic conductivity and wood density in Panamanian forest canopy trees. Oecologia **140,** 543–550.

Savi T, Marin M, Luglio J, Petruzzellis F, Mayr S, Nardini A. 2016. Leaf hydraulic vulnerability protects stem functionality under drought stress in *Salvia officinalis*. Functional Plant Biology **43,** 370–379.

Scoffoni C, McKown AD, Rawls M, Sack L. 2012. Dynamics of leaf hydraulic conductance with water status: quantification and analysis of species differences under steady state. Journal of Experimental Botany **63,** 643–658.

Scoffoni C, Sack L. 2015. Are leaves 'freewheelin'? Testing for a Wheeler-type effect in leaf xylem hydraulic decline. Plant, Cell and Environment **38,** 534–543.

Scoffoni C, Vuong C, Diep S, Cochard H, Sack L. 2014. Leaf shrinkage with dehydration: coordination with hydraulic vulnerability and drought tolerance. Plant Physiology **164,** 1772–1788.

Sperry JS. 2000. Hydraulic constraints on plant gas exchange. Agricultural and Forest Meteorology **104,** 13–23.

Trifilò P, Gascó A, Raimondo F, Nardini A, Salleo S. 2003*a*. Kinetics of recovery of leaf hydraulic conductance and vein functionality from cavitation-induced embolism in sunflower. Journal of Experimental Botany **54,** 2323–2330.

Trifilò P, Nardini A, Lo Gullo MA, Salleo S. 2003*b*. Vein cavitation and stomatal behaviour of sunflower (*Helianthus annuus*) leaves under water limitation. Physiologia Plantarum **119,** 409–417.

Tyree MT, Cochard H, Cruiziat P, Sinclair B, Ameglio T. 1993. Drought-induced leaf shedding in walnut: evidence for vulnerability segmentation. Plant, Cell and Environment **7,** 879–882.

Voicu MC, Cooke JEK, Zwiazek JJ. 2009. Aquaporin gene expression and apoplastic water flow in bur oak (*Quercus macrocarpa*) leaves in relation to the light response of leaf hydraulic conductance. Journal of Experimental Botany **60,** 4062–4075.

Xiong D, Yu T, Zhang T, Li Y, Peng S, Huang J. 2015. Leaf hydraulic conductance is coordinated with leaf morpho-anatomical traits and nitrogen status in the genus *Oryza*. Journal of Experimental Botany **66,** 741–748.

Zhu Y, Chang J, Huang S, Huang Q. 2016. Characteristics of integrated droughts based on a nonparametric standardized drought index in the Yellow River Basin, China. Hydology Research **47,** 454–467.